Density-functional theory for inhomogeneous fluids: Adsorption of binary mixtures

E. Kierlik and M. L. Rosinberg
Laboratoire de Structure et Reactivité aux Interfaces, Université Pierre et Marie Curie, Bâtiment F, 4 place Jussieu, 75230 Paris CEDEX 05, France
(Received 21 February 1991)

The nonlocal-density-functional theory for hard-sphere mixtures proposed in an earlier paper [Phys. Rev. A **42**, 3382, (1990)] is used to investigate the structure and the thermodynamics of binary simple liquid mixtures adsorbed on substrates. We study (i) the adsorption of Lennard-Jones fluids in slit-shaped pores with varying pore size, (ii) the selective adsorption of liquid argon-methane mixtures onto a planar graphite surface at constant pressure, (iii) the density profiles of charged hard spheres in the vicinity of a highly charged hard wall (primitive model of the electrical double layer). We compare our calculations to computer-simulation data and to the predictions of other recent theories. In all cases, packing effects are very well described by the theory, and most discrepancies can be ascribed to the mean-field treatment of attractive forces.

PACS number(s): 61.20.Gy, 68.45.−v, 05.70.−a

I. INTRODUCTION

The extensive use of computer simulations and the development of density-functional (DF) theory during the past decade have significantly improved our understanding of the physical processes involved in solid-fluid interfacial phenomena [1–5]. In particular, a comprehensive picture of the complex thermodynamic behavior of fluids in confined geometries is now available [6]. Comparison of the theoretical calculations with simulation results shows that DF theories are generally able to give a good qualitative description of the thermodynamics of these systems and predict correctly a large variety of possible phase transitions (wetting, prewetting, layering, capillary condensation, etc.). The most sophisticated versions of DF theory, which treat the short-ranged repulsive part of the intermolecular potential in a nonlocal fashion [7–12], can also describe successfully the microscopic structure of the fluids in the vicinity of solid surfaces, in particular the oscillatory behavior of the density profiles. In a preceding paper [13] (hereafter referred to as I) we proposed such a nonlocal DF for the inhomogeneous hard-sphere (HS) fluid and showed that it provides an accurate description of the adsorption of the pure fluid at a wall. This functional, which is essentially a simplified version of the one proposed recently by Rosenfeld [14,15], is based on the so-called smoothed (SDA) [8] or weighted (WDA) [9] density approximation like other nonlocal DF's used in the recent literature, but it has two major advantages over the other versions of the theory: first the weight functions are characteristic of each type of molecule, so that the application to multicomponent fluids is straightforward, and second these weight functions are purely geometric (i.e., density independent), which reduces considerably the computational effort required to minimize the free energy and to solve the corresponding Euler-Lagrange equations. Computational simplicity is an important aspect of the theory when dealing with multicomponent fluids. The main objective of the present work is therefore to test more thoroughly the predictions of the functional against existing simulations, in various situations where size (or packing) effects may play an important role: adsorption of fluids in micropores, selective adsorption from mixtures at constant pressure, and adsorption of electrolytes onto highly charged surfaces.

The remainder of the paper is arranged as follows. In the next section we briefly review the formalism and discuss the two-dimensional (2D) and one-dimensional (1D) limits of the theory: the behavior of a three-dimensional (3D) DF in these limits is a good indication of its performances for describing adsorption phenomena. For a more complete account of the theory the reader is referred to I and to recent papers of Rosenfeld [16]. Section III contains the results of our calculations and the comparison with simulations for Lennard-Jones fluids adsorbed in narrow slits. Emphasis is put on the determination of the solvation force which is now a measurable quantity. In Sec. IV theoretical predictions are compared to Monte Carlo simulations for liquid argon-methane mixtures adsorbed on graphite at constant pressure: in this case the relative surface excess as a function of the bulk composition is the relevant quantity for experiment. Section V is devoted to the study of the primitive model of the electrical double layer (charged hard spheres in a dielectric continuum near a charged wall). Conclusions and comments are found in Sec. VI.

II. THEORY

A. Brief review

As the general framework of the DF formalism is now well known [5], we give here only a brief account of our version of the theory (more details can be found in I). Like most of the works in this field, the theory is based on the usual separation of fluid-fluid interactions into repulsive and attractive contributions. The latter are treated in the meanfield approximation, i.e., correlations

are neglected (however in Sec. V electrostatic contributions to the short-range part of the pair correlations will also be considered). The repulsive part of the intrinsic Helmholtz free energy is modeled by the free-energy functional of a reference hard-sphere fluid, so that the grand potential functional of a multicomponent fluid in the external potentials $v_i(\mathbf{r})$ is written as

$$\Omega[\{\rho_i\}]=F_{\rm HS}[\{\rho_i\}] + \tfrac{1}{2}\int\int d\mathbf{r}\,d\mathbf{r}'\rho_i(\mathbf{r})\rho_j(\mathbf{r}')\phi_{ij}^{\rm attr}(|\mathbf{r}-\mathbf{r}'|) + \int d\mathbf{r}\,\rho_i(\mathbf{r})[v_i(\mathbf{r})-\mu_i] , \quad (1)$$

where $\rho_i(\mathbf{r})$ and μ_i are, respectively, the number density and the chemical potential of component i, and $\phi_{ij}^{\rm attr}$ is the attractive part of the pair potential (summation over repeated indices is implicit throughout this paper).

The originality of our treatment is based on the calculation of the excess contribution to $F_{\rm HS}[\{\rho_i\}]$ which we write after Percus [17] and Rosenfeld [14–16] as

$$F_{\rm HS}^{\rm ex}[\{\rho_i\}]=kT\int d\mathbf{r}\,\Phi(\{n_\alpha(\mathbf{r})\}) , \quad (2)$$

where $kT\Phi$ is the Helmholtz excess free-energy density of the HS uniform fluid and

$$n_\alpha(\mathbf{r})=\int d\mathbf{r}'\rho_i(\mathbf{r}')\omega_i^{(\alpha)}(\mathbf{r}-\mathbf{r}') . \quad (3)$$

$\alpha=1,2,3,4$ are weighted densities. Φ is taken from the scaled-particle theory [18] (SPT) [or, equivalently, from the compressibility equation in the Percus-Yevick [19] (PY) theory]:

$$\Phi=-n_0\ln(1-n_3)+n_1n_2/(1-n_3) + (1/24\pi)n_2^3/(1-n_3)^2 , \quad (4)$$

where n_0,n_1,n_2,n_3 are the reduced variables of the SPT: $n_\alpha=\rho_i R_i^{(\alpha)}$, with $R_i^{(0)}=1$, $R_i^{(1)}=R_i$, $R_i^{(2)}=4\pi R_i^2$, and $R_i^{(3)}=\frac{4}{3}\pi R_i^3$.

The four weight functions $\omega_i^{(\alpha)}(r)$ are simply related to the successive derivatives of the Heaviside step function $\Theta(r)$:

$$\begin{aligned}\omega_i^{(3)}(r)&=\Theta(R_i-r) ,\\ \omega_i^{(2)}(r)&=\delta(R_i-r) ,\\ \omega_i^{(1)}(r)&=(1/8\pi)\delta'(R_i-r) ,\\ \omega_i^{(0)}(r)&=-(1/8\pi)\delta'(R_i-r)+(1/2\pi r)\delta''(R_i-r) .\end{aligned} \quad (5)$$

Therefore, this DF theory for the HS fluid looks like a generalization of the SPT free energy to nonuniform situations and, as stated before, the main difference from the other nonlocal approximations proposed in the current literature is the introduction of four density-independent weight functions related to the geometry of the individual spheres. Conceptually, this is a great simplification; there is no need to introduce *ad hoc* generalizations of the weight functions for mixtures as is the case in Tarazona's approximation [20] or in the WDA of Curtin and Ashcroft [21]. Moreover, in practice, one does not have to solve self-consistent equations for the weighted densities as in the WDA or in the Meister-Kroll-Groot recipe [10]. The main difference from the original Rosenfeld's treatment [14] is the use of *scalar* weight functions only, since the introduction of vectorial quantities seems an unnecessary complication. By construction, this HS functional generates the analytical PY pair direct correlation function $c_{ij}^2(r)$ in the uniform limit; we have shown in I that it also predicts a good triplet function $c^3(\mathbf{r},\mathbf{r}')$ for the pure fluid. Although the theory does not seem to describe correctly inhomogeneities of infinite spatial extent [$\rho(\mathbf{r})\neq\rho$ everywhere], as is the case for the HS solid, it is fairly accurate for the adsorption at a wall where the density inhomogeneity is finite. In particular the density profile of the HS fluid near a hard wall is almost perfectly reproduced, up to a bulk packing fraction $\eta\simeq 0.46$. The probable reason for this good performance is now explained.

B. One- and two-dimensional limits

The structure of a fluid adsorbed at a solid substrate bears some resemblance to that of a uniform system in lower dimensionality. This is especially true for fluids confined in narrow slits [8] (then $D\simeq 2$) or cylindrical micropores [22] ($D\simeq 1$), but also when they are strongly adsorbed at a planar surface ($D\simeq 2$). Therefore, as suggested by Tarazona and co-workers [8], the performance of a three-dimensional DF in such situations can be related to its ability to describe properly the two- or one-dimensional uniform fluids. We first consider the 2D limit of a HS fluid mixture with radii R_i and three-dimensional densities of the form

$$\rho_i(\mathbf{r})=\rho_i^{(2D)}\delta(z) , \quad (6)$$

where each $\rho_i^{(2D)}$ is a two-dimensional uniform density

$$\rho_i^{(2D)}=\frac{1}{A}\int d\mathbf{r}\,\rho_i(\mathbf{r}) ,$$

where $A=\int\int dx\,dy$ is the area in the x-y plane. The calculation of the corresponding weighted densities from Eqs. (3) and (5) is straightforward and the excess free energy can be obtained from Eq. (2) via elementary integrations. The resulting expression for a mixture with unequal sizes is rather lengthy so we only give here the result for the one-component fluid. The excess free-energy density per particle is

$$\Phi^{(2D)}/\rho^{(2D)}=(1-\tfrac{2}{3}\eta^{(2D)}/(1-\eta^{(2D)})\{\eta^{(2D)}+[\eta^{(2D)}/(1-\eta^{(2D)})]^{1/2}\arctan[\eta^{(2D)}/(1-\eta^{(2D)})]^{1/2}\} , \quad (7)$$

where $\eta^{(2D)}=\pi R_i^2\rho_i^{(2D)}$ is the 2D packing fraction.

The numerical results are compared in Table I with those obtained from the accurate scaled-particle theory for hard disks [18]:

$$\Phi^{(2D)}/\rho^{(2D)}=\eta^{(2D)}/(1-\eta^{(2D)})-\ln(1-\eta^{(2D)}) , \quad (8)$$

and also with the predictions of Tarazona's functional [8]. The overall agreement is surprisingly good and in

TABLE I. Excess free-energy density per particle for hard disks as a function of the packing fraction $\eta^{(2d)}$. The result in the 2nd, 3rd, and 4th columns correspond to the present theory, the scaled particle theory (Ref. [18]), and Tarazona's SDA (Ref. [8]), respectively.

$\eta^{(2d)}$	$\Phi^{(2d)}/\rho^{(2d)}$ [Eq. (7)]	$\Phi^{(2d)}/\rho^{(2d)}$ [Eq. (8)]	$\Phi^{(2d)}/\rho^{(2d)}$ (SDA)
0.05	0.104	0.104	0.105
0.1	0.215	0.216	0.220
0.2	0.468	0.473	0.492
0.3	0.777	0.785	0.840
0.4	1.172	1.177	1.314
0.5	1.714	1.693	2.014
0.6	2.528	2.416	3.195
0.7	3.936	3.537	5.794

any case much better than for Tarazona's approximation. Good results are also obtained for asymmetrical mixtures when the size ratio is less than 2. Therefore we may be confident in the ability of the theory to describe correctly packing effects in quasi-2D regimes. Note that the structure of the hard-disk fluid (for instance the pair direct correlation function) can be also derived easily from the functional and that other interesting cases such as hard disk mixtures with nonadditive diameters can also be studied analytically by a similar procedure [23].

We now consider the 1D limit with three-dimensional densities of the form

$$\rho_i(\mathbf{r})=\rho_i^{(1D)}\delta(x)\delta(y) , \tag{9}$$

where $\rho_i^{(1D)}=(1/L)\int d\mathbf{r}\,\rho_i(\mathbf{r})$ is now a one-dimensional uniform density and $L=\int dz$ is the length in the z direction. Calculation of the corresponding weighted densities is again straightforward but the excess free energy is now infinite: $n_0(r)$ and $n_1(r)$ have nonintegrable singularities at $r=R_i$. Therefore the functional cannot describe correctly the 1D limit. This is unfortunate since Tarazona's SDA also fails in this regime [22]: the description of very small cylindrical pores remains a difficult challenge for any 3D density functional. Although that does not mean that our DF is totally inadequate for describing the behavior of fluids in cylindrical geometry, we shall only consider in Sec. III the case of slitlike pores.

III. ADSORPTION IN NARROW SLITLIKE PORES

The adsorption of fluids in porous materials has been a domain of very active research for a long time because of important applications in industry. Significant advances on the theoretical side have been made during the past decade (see [6] for a recent review on the subject) and this is a domain where DF theories have proved to be extremely useful. Because of the difficulty in describing real porous solids at the microscopic level, most theoretical studies have considered only highly idealized systems, such as single slits or cylinders of infinite length. The slitlike geometry is approximately realized in the well-known experiments of Israelachvili and co-workers [24] where the relevant quantity is the so-called solvation force (per unit area) f_s defined by [25]

$$f_s=-2\left[\frac{\partial\gamma}{\partial H}\right]_{\mu_i,T} , \tag{10}$$

where $\gamma=\frac{1}{2}(\partial\Omega/\partial A)_{V,T,\mu_i,H}$ is the plate-fluid interfacial tension, A is the surface area of each plate, and H is the separation between the plates (we put aside the direct van der Waals interaction between the material of the two walls). The solvation force $f_s(H)$ vanishes in the limit $H\to\infty$ and for small plate separations it shows oscillations which are due to the packing of the molecules confined by the walls. From the preceding discussion we expect that this force should be accurately determined by our density functional. We first consider the case of a pure fluid.

A. Adsorption of a pure fluid

In order to compare our theoretical predictions to available computer simulations we shall study the adsorption of a Lennard-Jones fluid with pair potential $\phi_{LJ}(r)=4\varepsilon[(\sigma/r)^{12}-(\sigma/r)^6]$ (which may be truncated and shifted at $r=r_c$ in some cases) and confined between two identical structureless walls by a 10-4-3 solid-fluid potential simulating the interaction with the basal plane of a graphite surface [26]:

$$\phi_{sf}(z)=2\pi\rho_s\varepsilon_{sf}\sigma_{sf}^2\Delta\{\tfrac{2}{5}(\sigma_{sf}/z)^{10}-(\sigma_{sf}/z)^4 -\sigma_{sf}^4/[3\Delta(0.61\Delta+z)^3]\} , \tag{11}$$

where ρ_s and Δ characterize the solid surface and ε_{sf} and σ_{sf} the solid-fluid potential. The cross parameters ε_{sf} and σ_{sf} are calculated via the Lorentz-Berthelot mixing rules. The other important interfacial quantity is the excess adsorption per unit area which we define here as

$$\Gamma^*=\Gamma\sigma^2=\tfrac{1}{2}\int_0^{H^*}[\rho^*(z^*)-\rho^*]dz^* , \tag{12}$$

where $z^*=z/\sigma$, $H^*=H/\sigma$, and $\rho^*=\rho\sigma^3$. This choice means that we take the Gibbs surface at the plane where ϕ_{sf} becomes infinite. The mean pore density is then $\rho_p^*=\rho_p\sigma^3=2\Gamma^*/H^*+\rho^*$ and the number of particles in the pore per unit area is $N^*=N\sigma^2=\rho_p^*H^*$. With these definitions, the thermodynamics of the confined system can be summarized by the following Gibbs adsorption equation:

$$2\,d\gamma+2s\,dT+2\Gamma\,d\mu+f_s dH=0 , \tag{13}$$

where s is the surface excess entropy per unit area.

We notice here that the choice of the relevant thermodynamic variable (μ, ρ, or p) for comparing simulation results to theoretical predictions is not obvious, because of the underlying differences in the bulk equation of state, which is only given approximately by the mean-field theory. Although the knowledge of μ is sufficient to obtain the density profile in a DF calculation, we think that it is preferable to use ρ (i.e., the density of the uniform fluid at the chemical potential fixed by the reservoir) as the input of the theory when varying the plate separation.

Then, one is sure to recover the correct limit of the density profile at large separations. Moreover, it is ρ (or the mole fractions for a mixture) which is actually controlled in the course of the experiments. On the other hand, the correct value of the density may not always be available from the simulation or easily calculated from an equation of state, especially in the case of mixtures [27].

Since we are dealing with an approximate theory, the choice of the equivalent hard-sphere diameter is not indifferent to the numerical predictions. Like most authors, we choose to split the fluid-fluid potential at the minimum $\sigma_{\min}=2^{1/6}\sigma$ in a Weeks-Chandler-Andersen (WCA) fashion [28], which defines the short-ranged part of the pair potential $\phi^{\text{rep}}=\phi-\phi^{\text{attr}}$. Then, according to WCA, the equivalent hard-sphere diameter d should be temperature and density dependent. A good approximation of d is given by the Barker-Henderson [29] expression

$$d=d(T)=\int_0^{\sigma_{\min}}\{1-\exp[-\beta\phi^{\text{rep}}(r)]\}dr\ , \qquad (14)$$

which is only temperature dependent. However, there is no reason why this choice should be adequate when dealing with arbitrary nonuniform situations since an optimization principle is no longer available. In particular, for the high densities which occur near adsorbing surfaces, the value of d given by Eq. (14) may be overestimated. Another possible choice for d, which appears to yield better results for supercritical or near-critical adsorption [30], is the one suggested by Lu, Evans, and Telo da Gama [31]:

$$d(T)/\sigma=(\alpha_1 T^*+\alpha_3)/(\alpha_2 T^*+1)\ , \qquad (15)$$

where $\alpha_1=0.3837$ and $\alpha_2=0.4293$ (as given by Verlet and Weis [32]) and α_3 is a free parameter chosen such that the theory yields a good fit of the liquid density along the coexistence curve. A modification of ϕ_{attr} has also been suggested by some authors [33–35] to improve the bulk equation of state given by the mean-field theory. We shall not consider this last possibility in the present paper.

To illustrate the influence of the choice of d on the predictions of the theory, we first compare the DF theoretical results with simulated results mimicking the adsorption of a supercritical LJ fluid on graphite at temperature $T^*=1.35$ in a slit of width $H^*=5$. This system has been first studied by van Megen and Snook [36] in a grand canonical ensemble Monte Carlo (GCEMC) simulation and calculations have been repeated by Walton and Quirke [37] and more recently by Tan and Gubbins [30]. Density-functional results are also available [38]. Calculations were carried out with parameters for the fluid modeling approximately ethylene (see Table II) and with the solid-fluid parameters actually used by van Megen and Snook and the other authors: $\sigma_{sf}=0.3809$ nm ($\sigma_s=0.340$ nm), $2\pi\rho_s\varepsilon_{sf}\sigma_{sf}^2\Delta=12.96\varepsilon$, $\Delta=0.3393$ nm. The cutoff radius for the LJ potential was $r_c=2.5\sigma$ and we found that a good fit of the liquid densities at coexistence was obtained with $\alpha_3=1.032$ in Eq. (15) [the Verlet-Weis [32] fit to Eq. (14) corresponds to $\alpha_3=1.068$]. The density profile in the slit is compared to the simulation in Fig. 1 at $\mu^*=\mu/\varepsilon=-3$, which fixes the bulk density $\rho^*=0.28$. We see that choosing the value of d from Eq. (15) ($d=0.4136$ nm) instead of Eq. (14) ($d=0.4236$ nm) improves the agreement, which is good in both cases anyway. The improvement is more apparent for the mean pore density ρ_p which is an integrated quantity: we find $\rho_p^*=0.568$, to be compared to $\rho_p^*(MC)=0.564$ instead of $\rho_p^*=0.521$ when d is taken from Eq. (14). The excess adsorption isotherm (Γ^* as a function of ρ^*) shown in Fig. 2 confirms that this slight modification of the value of d is not indifferent to the success of the theory. For the system and the conditions considered here, the performance of our DF is comparable to Tarazona's SDA, as tested by Tan and Gubbins [30] who also adjusted the hard-sphere diameter according to Eq. (15). We remark the pronounced maximum in the isotherm, which is characteristic of the adsorption of fluids at supercritical temperatures.

Snook and van Megen [39] have been the first to carry out a systematic study of the density profile and of the solvation force as a function of the plates separation H. Their GCEMC calculations have been confirmed and completed by Magda, Tirell, and Davis [40] in a later

TABLE II. Interaction parameters for the Lennard-Jones potentials.

	C_2H_4	Ar	Kr	CH_4
σ (nm)	0.4218	0.3405	0.3630	0.3817
ε/k (K)	201.8	119.8	163.1	148.2

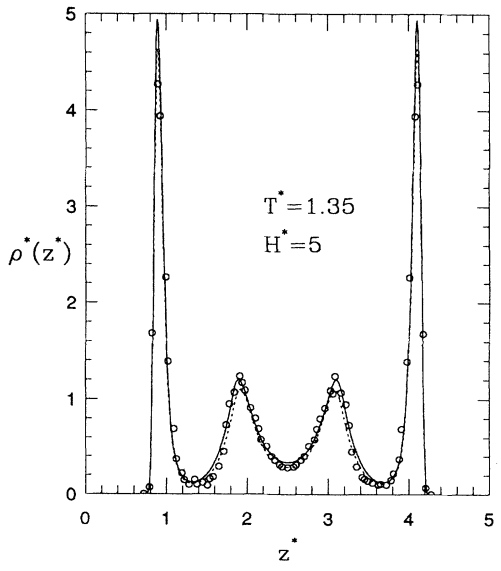

FIG. 1. Density profile for ethylene in a carbon slitlike pore of width $H^*=5$ at $T^*=1.35$. The theoretical results are shown by dashed [using d from Eq. [14)] and solid [using d from Eq. (15)] lines, while simulation results (from Ref. [37]) are shown as circles.

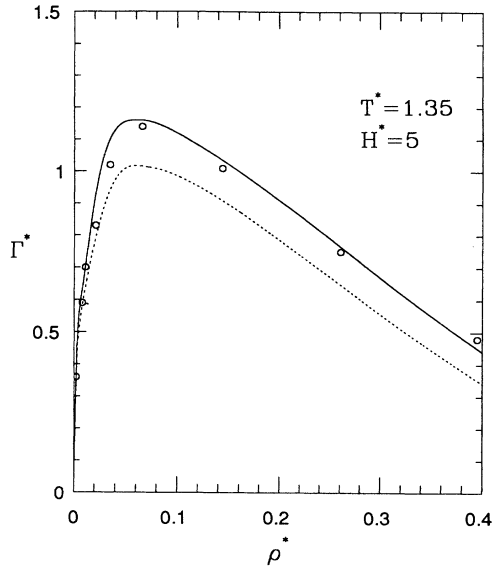

FIG. 2. Excess adsorption isotherm per unit area of ethylene in a carbon slitlike pore of width $H^*=5$ at $T^*=1.35$. The theoretical results are shown by dashed [using d from Eq. (14)] and solid [using d from Eq. (15)] lines, while simulation results (from Ref. [30]) are shown as circles.

molecular-dynamics simulation (MD). In this study, the solid atoms are chosen identical to the fluid molecules ($\sigma_s=\sigma$, $\varepsilon_s=\varepsilon$) and values of $\Delta=1/\sqrt{2}\sigma$ and $\rho_s\sigma_{sf}^2\Delta=1$ are assumed. The liquid is characterized by the reduced temperature $T^*=1.2$ and the reduced chemical potential $\mu^*=-2.477$ ($\mu_{ex}^*=\mu^*-T^*\ln\rho^*=-1.849$). According to Snook and van Megen [39], the corresponding reduced bulk density and bulk pressure are $\rho^*=0.5925$ and $p^*=p\sigma^3/\varepsilon=0.24$ (with $r_c=3.5\sigma$). This situation corresponds approximately to a bulk liquid under its own vapor pressure. The theoretical density profiles are compared to the simulation results (*at the same bulk density*) for $H^*=3$, 4, and 7.5 in Figs. 3–5. The agreement is excellent in the three cases. We have taken the value of d from Eq. (15) ($d/\sigma=0.984$) instead of Eq. (14) ($d/\sigma=1.009$) and again this choice improves significantly the results for the integrated quantities, especially at large separations (the theoretical bulk pressure and excess chemical potential are $p^*=0.177$ and $\mu_{ex}^*=-3.101$, respectively). The comparison for these quantities is presented in Table III. The reduced solvation force $f_s^*=f_s\sigma^3/\varepsilon$ has been calculated from the microscopic expression [25]

$$f_s=-\int_0^H \frac{d\phi_{sf}(z)}{dz}\rho(z)dz-p\ , \tag{16}$$

which is equivalent to Eq. (10) (actually, the comparison between the results computed from the two expressions of f_s can be used to test the accuracy of the calculations). Note that Snook and van Megen [39] and Magda, Tirell, and Davis [40] refer to the first term on the right-hand side of Eq. (16) as the solvation force and $-2(\partial\gamma/\partial H)_{\mu,T}$ is then termed the disjoining pressure $\Pi(H)$, as introduced by Derjaguin [41]. The variations of f_s as a function of the plate separation are compared to the simulations in Fig. 6 (the underlying physics is now well known

TABLE III. LJ fluid in a 10-4-3 slitlike pore at $T^*=1.2$ ($\rho^*=0.5925$): thermodynamic quantities as a function of the pore width. Γ^*, N^*, γ^*, and f_s^* are the reduced excess adsorption, the number of particles in the pore per unit area, the interfacial tension, and the solvation force, respectively. The numbers in parentheses are the MD results of Magda, Tirell, and Davis (Ref. [40]).

H^*	Γ^*	N^*	$2\gamma^*$	f_s^*
2.25	−0.281	0.772	−2.90	−2.773
	(−0.28)	(0.77)	(−2.86±0.13)	(−2.88±0.04)
2.5	−0.318	0.845	−2.50	−0.626
	(−0.33)	(0.82)	(−2.46±0.05)	(−0.66±0.01)
2.75	−0.203	1.224	−3.02	4.053
	(−0.18)	(1.27)	(−2.91±0.05)	(4.67±0.01)
3	−0.164	1.450	−3.62	0.313
	(−0.17)	(1.45)	(−3.28±0.17)	(0.24±0.06)
3.2	−0.206	1.484	−3.45	−1.192
	(−0.21)	(1.48)	(−3.37±0.15)	(−1.29±0.01)
3.5	−0.227	1.620	−3.19	−0.061
	(−0.25)	(1.57)	(−2.85±0.08)	(−0.25)
3.75	−0.155	1.911	−3.35	1.179
	(−0.15)	(1.92)	(−3.46±0.14)	(1.40±0.1)
4	−0.141	2.088	−3.51	0.076
	(−0.14)	(2.10)	(−3.52±0.09)	(0.13±0.1)
6	−0.123	3.309	−3.54	0.014
	(−0.12)	(3.32)		(0.08)
7.5	−0.120	4.205	−3.56	0.007
	(−0.12)	(4.2)		(−0.03)
9.5	−0.117	5.395	−3.53	0.004
	(−0.12)	(5.4)		(−0.07±0.08)

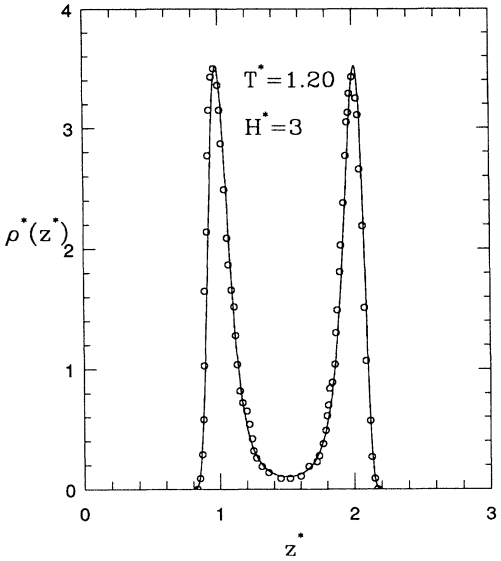

FIG. 3. Density profile for a Lennard-Jones fluid in a slit of width $H^*=3$ at $T^*=1.20$. The theoretical results are shown by solid lines, while simulation results (from Ref. [40]) are shown as circles.

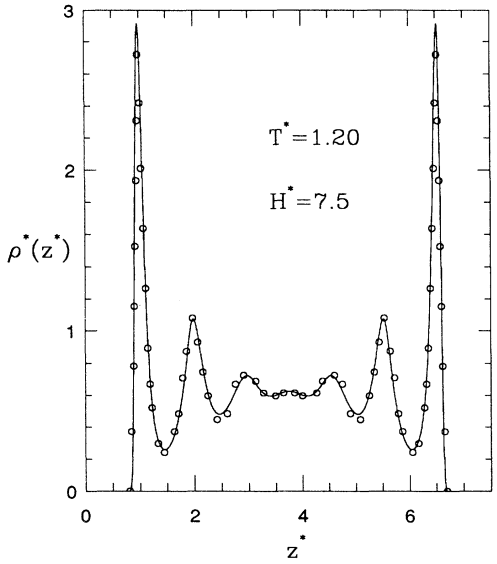

FIG. 5. Same as in Fig. 3, but in a slit of width $H^*=7.5$ (simulation results are taken from Ref. [39]).

and there is no need to repeat here the arguments): the overall agreement is good and the discrepancies can be attributed to the disagreement between the values of the bulk pressure ($p^*=0.177$ instead of 0.24) and to the small deviations in the density profiles, which are not visible at the scale of Figs. 3–5 but contribute significantly to f_s in Eq. (16), because of the multiplication by the gradient of the solid-fluid potential.

Anyhow, the global accuracy of the theory in this problem is remarkable: the *quantitative* agreement with the simulations for the density profiles is comparable to what has been recently obtained by Kjellander and Sarman [42] via the integral equation technique with a closure at the level of the anisotropic pair distribution function. But this technique requires a much larger computational effort than the present DF calculations and thermodynamical quantities (as for instance the interfacial tension) are not directly accessible. The present version of the DF theory is certainly more accurate than the other versions tested by Vanderlick, Scriven, and Davis [11],

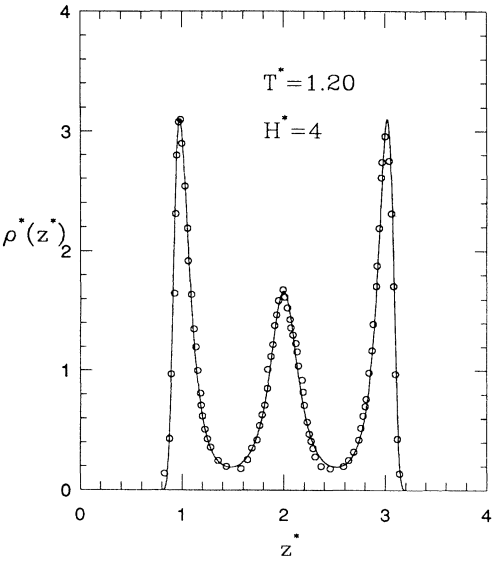

FIG. 4. Same as in Fig. 3, but in a slit of width $H^*=4$.

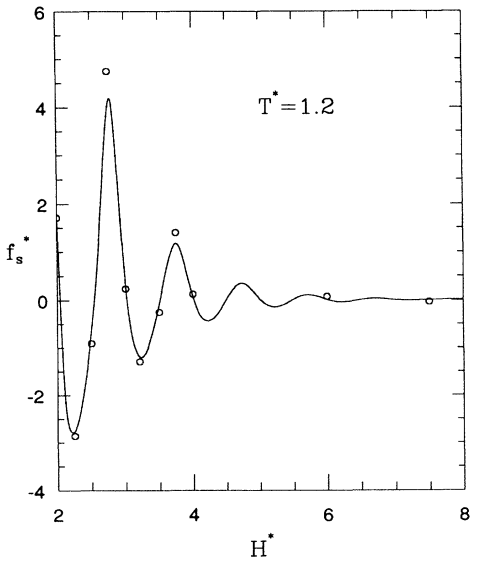

FIG. 6. Solvation force for a Lennard-Jones fluid in slits of width H^* at $T^*=1.2$. The theoretical results are shown by solid lines, while simulation results (from Ref. [40]) are shown as circles.

Tarazona's model included (note however that Vanderlick, Scriven, and Davis do not split the intermolecular potential according to the WCA recipe). We believe that most discrepancies with the computed results can be ascribed to the use of the mean-field approximation.

We now consider the application of the theory to the case of fluid mixtures in slitlike pores.

B. Adsorption of a binary mixture

Theoretical studies of the adsorption of fluid mixture at substrates are still in their infancy and only few simulations in model pores have been performed [27,43,44]. As a test, we shall compare our DF calculations to the recent MD simulations of Sokolowski and Fischer [27] who considered argon/krypton mixtures confined in slitlike pores by a (9,3) LJ potential, which is also appropriate to represent graphite walls [26]:

$$\phi_{sf}(z)=(3\sqrt{3}/2)\varepsilon_{sf}[(\sigma_{sf}/z)^9-(\sigma_{sf}/z)^3] . \quad (17)$$

The parameters used for Ar (1) and Kr (2) are given in Table II (with no cutoff). The solid-fluid potential parameters are $\sigma_{s1}/\sigma_1=0.5621$, $\sigma_{s2}/\sigma_1=0.588$, $\varepsilon_{s1}/\varepsilon_1=9.2367$ and $\varepsilon_{s2}/\varepsilon_1=12.1744$. We have calculated the density profiles at the supercritical temperature $T^*=kT/\varepsilon_1=2$ and for the total reduced density $\rho^*=(\rho_1+\rho_2)\sigma_1^3=0.444$ and the mole fraction of Ar $x_1=\rho_1/(\rho_1+\rho_2)=0.262$ in a pore of width $H^*=H/\sigma_1=5$. In this example we have simply used the Barker-Henderson hard-sphere diameters obtained from Eq. (14). The comparison to the MD results is presented in Fig. 7 (note that the profiles are drawn here for half of the slit). The corresponding excess adsorptions for Ar and Kr are $\Gamma_1^*=\Gamma_1\sigma_1^2=-0.067$ and $\Gamma_2^*=\Gamma_2\sigma_1^2=0.213$, respectively, to be compared to the MD results $\Gamma_1^*=-0.07$ and $\Gamma_2^*=0.26$. It is important to remark that the densities ρ_1 and ρ_2 have been determined by Sokolowski and Fischer using the chemical potentials obtained in the simulation by the test particle method to solve the equation of state of the mean-field theory. As pointed out before, this may be a serious source of error in the comparison of the simulation with the theory and it would have been preferable to perform the DF calculations with the "exact" densities of the surrounding bulk medium. This problem may explain some of the discrepancies observed in the excess adsorptions. Nevertheless, the overall agreement is fairly good and the performance of our functional for this system is comparable to the Meister-Kroll-Groot [10] (MKG) approach tested by Sokolowski and Fischer. This DF theory also requires much more laborious numerical computations than the present one, in particular for obtaining the weighted densities.

Sokolowski and Fischer, like other authors [6], have concentrated on the determination of the capillary phase diagram of the confined fluid and the calculation of adsorption isotherms at fixed pore width. We do not expect the MKG results to be *significantly* modified by the present theory and we must be aware that the description of the thermodynamics inside pores (especially the determination of the critical temperatures) is rather sensitive to the mean-field character of the theory. However, there are some differences between the two theories which may be noticed: for instance, at $T^*=1.5$ and $H^*=5$, we observe continuous adsorption isotherms for all bulk fluid composition, as predicted by the simulation. On the other hand, the MKG theory yields capillary condensation

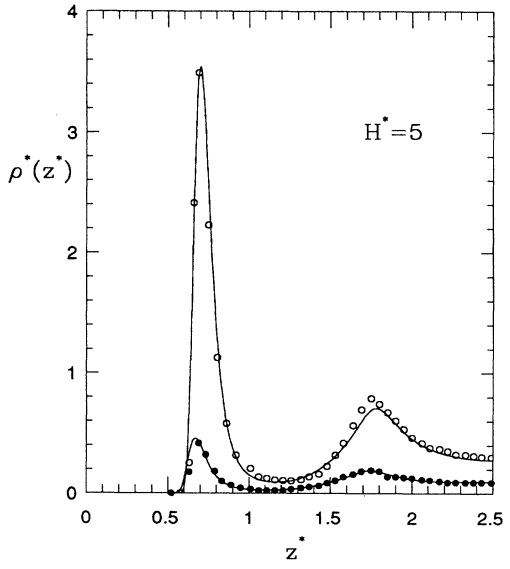

FIG. 7. Density profiles for an argon-krypton mixture adsorbed in a graphite slitlike pore of width $H^*=5$ at $T^*=2$ (dimensionless quantities are in terms of the argon parameters). The total density and the mole fraction of argon are $\rho^*=0.444$ and $x_1=0.262$, respectively. The theoretical results are shown by solid lines, while simulation results (from Ref. [27]) are shown as solid (Ar) and open (Kr) circles.

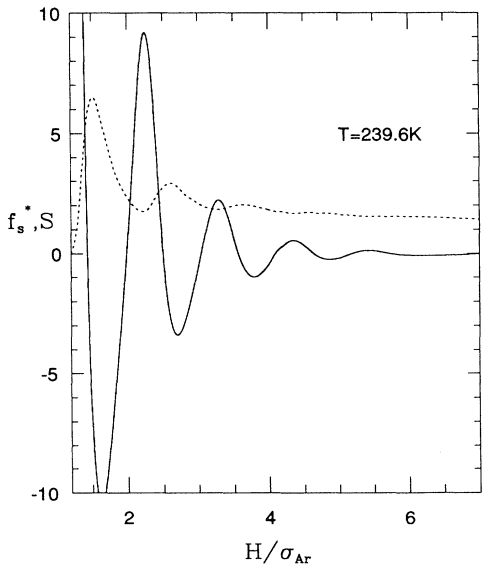

FIG. 8. Theoretical predictions for the solvation force (solid line) and the selectivity (dashed line) for the same system as in Fig. 7.

when the mole fraction of argon is less than 0.09. The critical temperature inside the pore is therefore better estimated with our treatment of short-ranged forces.

We wish also to look at the changes in the fluid structure as a function of the pore width, at fixed bulk concentration and composition. In Fig. 8, we plot the solvation force and the selectivity of krypton relative to argon versus the pore width, for the same system considered previously at $T^*=2$. In the case of mixtures the solvation force is just the sum of the forces due to each component [25], and the selectivity (or separation factor) of component 2 relative to component 1 is defined as [45]

$$S=[(1-y_1)/y_1]/[(1-x_1)/x_1]\ , \tag{18}$$

where $y_1=\rho_p^1/(\rho_p^1+\rho_p^2)$ is the mole fraction of component 1 in the pore. This quantity is important for practical applications since it indicates the ability of a porous adsorbent to separate the different constituents of the mixture. The selectivity approaches asymptotically to unity as the pore width goes to infinity and the oscillating behavior at small separations is related to the layering structure and the packing effects in the confined fluid, as for the solvation force. A similar behavior has been observed by Tan *et al.* in their recent DF calculations [44] based on an extension to mixtures of Tarazona's SDA [20]. In the present case krypton is preferentially adsorbed, reflecting the stronger interaction with the graphite surface ($\varepsilon_{s2}>\varepsilon_{s1}$), but the selectivity is much smaller than the one found by Tan *et al.* because we have considered a rather high temperature which smooths the differences between the two components of the mixtures. However, at very small separations, size effects play a determinant role and since argon molecules can penetrate into the pore more easily than krypton, the selectivity falls to zero. In consequence, at fixed temperature and bulk composition, the selectivity passes through a maximum for a certain pore size ($H\sim 0.52$ nm), which then would be an optimum choice from the point of view of fluids separation. Of course, this example is mainly illustrative and we must not forget that we have neglected the lateral structure of the graphite walls, which may change the quantitative predictions for the smallest pores and lower temperatures [30].

IV. SELECTIVE ADSORPTION FROM A BINARY LIQUID MIXTURE AT CONSTANT PRESSURE

In a large class of experiments selective adsorption from fluid mixtures onto solid surfaces is studied *at constant pressure* by measuring the composition of the adsorbate phase as the bulk composition of the fluid is varied [46]. Many efforts have been devoted to the prediction of multicomponent adsorption equilibria from the knowledge of pure-component adsorption isotherms, in relation to the design of separation processes [45]. Since the thermodynamics of multicomponent adsorption is most often based on the assumption that adsorbed fluid mixtures behave like ideal or regular solutions [46,47], the primary objective of statistical mechanical methods is to test the validity of these approximations on model interfaces well defined at the microscopic level. Then, in a second state, one may hope that these methods will be useful in the case of real solid-fluid interfaces with strong deviations from ideality.

Monte Carlo simulations in the isobaric-isothermal ensemble (NPTMC) are especially appropriate for the study of adsorption from mixtures. Such a method has been recently developed by Finn and Monson [48] and applied to the study of selective adsorption of model vapor and liquid mixtures of argon and methane on graphite [49]. In the following, we shall compare their simulation results to the predictions of the DF theory in the case of liquids. Vapor mixture adsorption will be studied in more details in a subsequent paper. The graphite surface is again represented by the 10-4-3 Steele potential (with $\sigma_s=\Delta=0.340$ nm, $\varepsilon_s/k=28.0$ K, $\rho_s=112.26$ nm^{-3}) and the fluid-fluid potentials for methane and argon (see Table II) are truncated at $r_c=2.5\sigma_{CH_4}$ with no tail corrections. As noted by Finn and Monson [49], CH_4-Ar mixtures are reasonably ideal, so that their bulk thermodynamic properties can be accurately described by the van der Waals one-fluid theory [50]. This provides a simple way of computing the bulk densities at a given composition, from the knowledge of the pressure used in the simulation. On the other hand, the choice of these densities as the input of the theory means that the pressure obtained from the mean-field equation of state will not stay constant as the bulk composition is varied. Therefore one must check *a posteriori* that the variations of p remain acceptable. Calculations have been performed at $T^*=0.8$ and $p^*=0.04$ (dimensionless quantities are in terms of the methane parameters), which give a quite dense liquid mixture. The equivalent hard-sphere diameters have been computed from Eq. (14). The density profiles corresponding to the bulk compositions $x_1=x_{CH_4}=0.19$ and 0.60 are shown in Figs. 9 and 10, re-

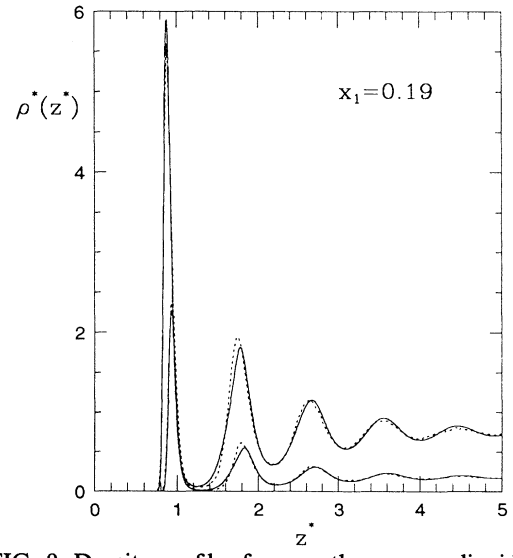

FIG. 9 Density profiles for a methane-argon liquid mixture adsorbed on graphite at $T^*=0.8$ (dimensionless quantities are in terms of the methane parameters). The bulk pressure and the mole fraction of methane are $p^*=0.04$ (as given by the simulation) and $x_1=0.19$, respectively. The theoretical results are shown by solid lines, while simulation results (from Ref. [49]) are shown by dashed lines.

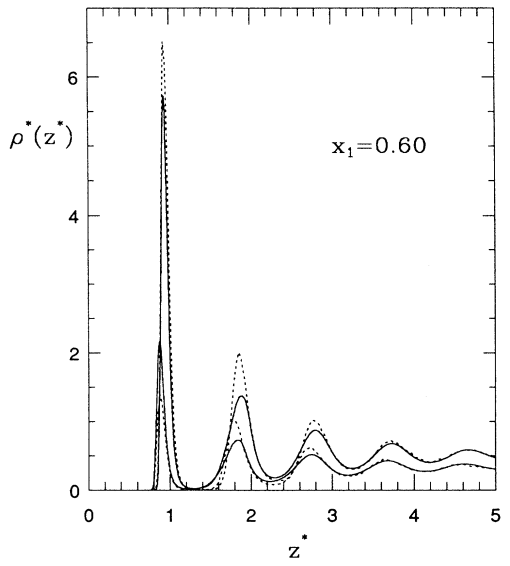

FIG. 10. Same as in Fig. 9, but for a mole fraction of methane $x_1=0.60$.

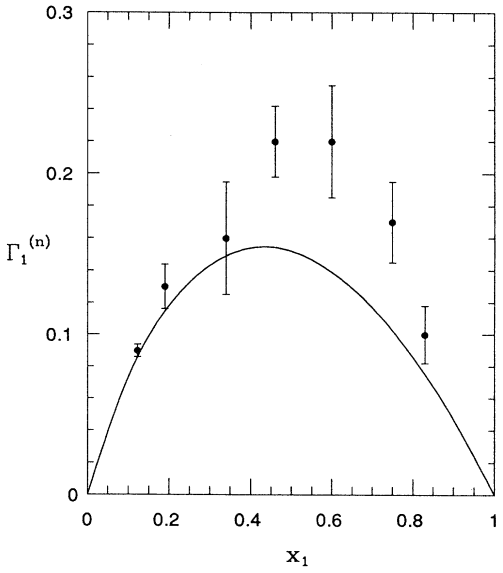

FIG. 11. Surface excess concentration of methane as a function of bulk composition for methane-argon liquid mixtures adsorbed on graphite at $T^*=0.8$ and $p^*=0.04$. The theoretical results are shown by solid lines, while simulation results (from Ref. [49]) are shown as solid circles.

spectively. It is clear that the predictions of the theory, which are good at $x_1=0.19$, deteriorate significantly as the concentration of methane increases. The mean-field pressure is quite far from the MC pressure and varies between $p^*=0.74$ and 1.06 as x_1 goes from 0 to 1. However the source of the problem is not in these variations and we have checked that keeping constant the pressure by adjusting the densities or that using the bulk densities obtained from the limit of the MC profiles far from the surface would lead only to minor changes in the theoretical predictions. In fact, the poorer agreement at the higher methane concentrations arises from the failure of the mean-field theory: this is not very surprising, because the temperature is near the triple point of methane and a higher methane concentration means stronger attractive forces in the liquid and with the surface. It is likely that the theory would be more accurate at a higher temperature. However, changing T in the calculations in order to have the same reduced temperature T/T_c as in the simulation [T_c(MC)=1.23, T_c(MFA)=1.32] does not improve the agreement. Attempts to adjust the hard sphere diameters have been unsuccessful too. The annoying consequence of this failure is that the surface excess concentration of methane $\Gamma_1^{(n)}=x_2\Gamma_1-x_1\Gamma_2$ is not predicted correctly in the whole domain of bulk composition, as shown in Fig. 11. This quantity is the primary function characterizing adsorption equilibrium in liquid mixtures and is readily obtained from the experiment once the specific surface area of the solid is known [46]. Both simulation and theoretical results show a small positive adsorption excess for methane due to the stronger interactions with the surface (note the large error bars in the simulated results which reflect the difficulty of computing excess properties). From the parabolic shape of the surface excess isotherm in Fig. 11 it is usually concluded that the mixture is close to ideality, both in the bulk and in the "adsorbed phase" [46]. This is precisely the kind of assumption which should be controlled by a statistical mechanical treatment and we intend to return to this problem in a future work.

V. APPLICATION TO THE THEORY OF THE ELECTRICAL DOUBLE LAYER

The last example of solid-fluid interface that we want to investigate in the present paper is the one corresponding to an electrolyte solution in the vicinity of a charged surface. Because of the ubiquity of charged layers in physical chemistry or biology, considerable efforts have been devoted to the theoretical description of this interface and we refer the reader to one of the many reviews on the subject (for instance, [51]). A large part of the underlying physics is already contained in the so-called primitive model, in which ions are represented by charged hard spheres next to a uniformly charged planar wall, the whole system being immersed in a dielectric continuum. At high bulk concentrations and surface charge densities (which, incidentally, cannot be reached in real experiments), computer simulations in 1:1 electrolytes [52–54] show the formation of a second layer of counter ions next to the wall, which leads to a large value of the potential drop. The prediction of this phenomenon, which supposes a proper description of both electrostatic and packing effects in the inhomogeneous fluid, has been a challenge for all modern double-layer theories and sophisticated calculations have been performed in the recent years [53,55]. It is clear that nonlocal density functionals are also adequate to the treatment of this problem and this route has been taken by some authors [56,57]. Our approach is similar to the one proposed recently by Mier-y-Teran *et al.* [57] but we

suggest a slightly different derivation which we think is more transparent (in particular in the treatment of electrostatic contributions).

We consider the general situation where the electrolyte solution is enclosed in a macroscopic volume V with some external charges $q_s(\mathbf{r})$ adsorbed on the surface S. As usual when dealing with long-ranged Coulomb forces, it is convenient to consider the electrostatic contribution to the free energy separately [58], so that we write the grand thermodynamic potential for the total system [including the external charge $q_s(\mathbf{r})$] as

$$\Omega = G[\{\rho_i\}]+\tfrac{1}{2}\int d\mathbf{r}\, q(\mathbf{r})\Psi(\mathbf{r}) + \int d\mathbf{r}\,\rho_i(\mathbf{r})[v_i(\mathbf{r})-\mu_i]\ , \tag{19}$$

where G is a unique (but unknown) functional of the ionic densities $\rho_i(\mathbf{r})$, $v_i(\mathbf{r})$ is the nonelectrostatic part of the external potential, and $q(\mathbf{r})=e_i\rho_i(\mathbf{r})+q_s(\mathbf{r})$ is the total local charge density, related to the mean electrostatic potential $\Psi(\mathbf{r})$ through Poisson's equation

$$\Delta\Psi(\mathbf{r}) = -(4\pi/\varepsilon)q(\mathbf{r})\ , \tag{20}$$

where e_i is the charge of the ion of species i and ε is the dielectric constant of the medium. We may now rewrite Ω as follows:

$$\Omega = G[\{\rho_i\}]+\int d\mathbf{r}\, q(\mathbf{r})\Psi(\mathbf{r})-\varepsilon/8\pi\int d\mathbf{r}|\nabla\Psi(\mathbf{r})|^2 + \int d\mathbf{r}\,\rho_i(\mathbf{r})[v_i(\mathbf{r})-\mu_i]\ , \tag{21}$$

this formulation having the advantage that $\Psi(\mathbf{r})$ can be treated as a variable in the theory with the same status as $\{\rho_i\}$, so that requiring $\delta\Omega/\delta\rho_i(\mathbf{r})=0$ implies the Euler-Lagrange equations

$$\frac{\delta G}{\delta\rho_i(\mathbf{r})}+e_i\Psi(\mathbf{r})+v_i(\mathbf{r})=\mu_i \tag{22}$$

and requiring $\delta\Omega/\delta\Psi(\mathbf{r})=0$ implies the Poisson's equation [58]. Moreover, the boundary condition on $\Psi(\mathbf{r})$ on S can also be recovered by separating volume and surface terms [58]. At this stage, the approximation $G[\{\rho_i\}]=F_{\rm HS}[\{\rho_i\}]$ would correspond to a mean-field treatment of electrostatic interactions, analogous to the Gouy-Chapman theory [51], except that hard-sphere effects are now included. We know from Groot [56] that this first approximation is able to describe the formation of the second layer of counter ions, but the magnitude of the phenomenon is quite exaggerated. Therefore it is necessary to go a step further and to include in the correlations some contribution of the Coulomb interactions. This can be done rather simply by using the perturbative approach proposed by Curtin and Ashcroft [59] for calculating the freezing properties and the liquid-gas coexistence curve of the Lennard-Jones fluid. We first make a functional Taylor expansion of the excess part of $G[\{\rho_i\}]$ in powers of $\Delta\rho_i(\mathbf{r})=\rho_i(\mathbf{r})-\rho_i$ (ρ_i refers to the homogeneous neutral fluid far from the surface):

$$G^{\rm ex}[\{\rho_i\}]=G[\{\rho_i\}]-F_{id}[\{\rho_i\}] = \int d\mathbf{r}\, g^{\rm ex}(\{\rho_i\})+\tilde{\mu}_i^{\rm ex}\int d\mathbf{r}\,\Delta\rho_i(\mathbf{r}) -\frac{kT}{2}\int d\mathbf{r}\,d\mathbf{r}' c_{ij}^{sr}(|\mathbf{r}-\mathbf{r}'|) \times\Delta\rho_i(\mathbf{r})\Delta\rho_j(\mathbf{r}')-\cdots\ , \tag{23}$$

where we have used the relationships between the functional derivatives of $G^{\rm ex}$ and the non-Coulombic part of the direct correlation functions c_{ij}^{sr}, $c_{ijk}^{sr},\ldots$. $\tilde{\mu}_i^{\rm ex}=\mu_i^{\rm ex}-e_i\Psi(\text{bulk})$ is the contribution to the excess chemical potential arising from the non-Coulombic terms [58] and $g^{\rm ex}$ is the Helmholtz excess free-energy density of the uniform ionic mixture *minus* the electrostatic self-energy. We can write c_{ij}^{sr} as

$$c_{ij}^{sr}=c_{ij}^{\rm HS}+\Delta c_{ij}\ , \tag{24}$$

where $c_{ij}^{\rm HS}(\mathbf{r})$ is the direct correlation function of the corresponding uniform hard-sphere fluid (i.e., *at the same density* $\{\rho_i\}$). A similar formal separation can be performed on the direct correlation functions of all orders in Eq. (23). We now sum the hard-sphere contributions to all orders and neglect the higher-order terms $\Delta c_{ijk\ldots}^{(n)}$ ($n>2$). The result for G is

$$G[\{\rho_i\}]=F_{\rm HS}[\{\rho_i\}]+\int d\mathbf{r}[g(\{\rho_i\})-f_{\rm HS}(\{\rho_i\})] +(\tilde{\mu}_i-\mu_{i,\rm HS})\int d\mathbf{r}\,\Delta\rho_i(\mathbf{r}) -\frac{kT}{2}\int d\mathbf{r}\,d\mathbf{r}'\Delta c_{ij}(|\mathbf{r}-\mathbf{r}'|)\Delta\rho_i(\mathbf{r})\Delta\rho_j(\mathbf{r}')\ , \tag{25}$$

where $\{\mu_{i,\rm HS}\}$ and $f_{\rm HS}$ are the chemical potentials and the Helmholtz free-energy density of the uniform hard-sphere fluid, respectively. Finally, we can rewrite the Euler-Lagrange equations (22) for the equilibrium density profiles:

$$-kT\ln[\rho_i(\mathbf{r})/\rho_i]=v_i(\mathbf{r})+\left[\frac{\delta F_{\rm HS}^{\rm ex}}{\delta\rho_i(\mathbf{r})}-\mu_{i,\rm HS}^{\rm ex}\right] +e_i[\Psi(\mathbf{r})-\Psi(\text{bulk})] -kT\int d\mathbf{r}'\Delta c_{ij}(|\mathbf{r}-\mathbf{r}'|)\Delta\rho_j(\mathbf{r}')\ , \tag{26}$$

where $F_{\rm HS}^{\rm ex}$ is evaluated from Eq. (2).

So far we have not specified how to calculate the bulk properties of the fluid. There are many approximate theories available and the most widely used is the mean-spherical approximation (MSA) which is of reasonable accuracy while yielding analytical expressions for the direct correlation functions. In the case of the restricted primitive model (RPM) where all ions have the same diameter σ, one has [60]

$$kT\Delta c_{ij}(r)=\begin{cases}-(e_ie_j/\varepsilon)[2B/\sigma-(B/\sigma)^2r-1/r], & r<\sigma\\ 0, & r>\sigma,\end{cases} \tag{27}$$

where $B=x^{-2}[x^2+x-x(1+2x)^{1/2}]$ and $x^2=(\kappa\sigma)^2=[(4\pi/\varepsilon kT)\rho_i e_i^2]\sigma^2$, κ being the inverse Debye length. However, it is well known that the major deficiency of the MSA is its serious lack of thermodynamic consistency and this shortcoming may have significant consequences when the theory is used in interfacial situations [61]. We first note that in the RPM the chemical potential, the pressure or the free energy calculated from Eq. (27) via the compressibility equation are just the PY hard-sphere values, because of the spurious structure $\Delta c_{ij}(r)=-e_i e_j f(r)$. More seriously for the present purpose, the density profiles solution of Eqs. (20) and (26) at zero surface charge are identical to those of a neutral mixture of hard spheres near a hard wall. In order to overcome this problem, one should use more elaborated theories, for instance the generalized MSA (GMSA) [62], which is thermodynamically self-consistent and still analytical. However, like other authors [56,57], we shall only consider the MSA in the present work, as a first approximation. Our numerical procedure involves the simultaneous resolution of Eq. (26) by the standard Picard iteration method and of Eq. (20) by a predictor-corrector algorithm [since the field is known at $z=0$ we just guess $\Psi(0)$ until $\Psi(\infty)$ is less than tolerance] [63]. The accuracy of the calculations is controlled by checking two important sum rules, the so-called contact theorem [64]:

$$kT[\rho_+(0)+\rho_-(0)]=p+2\pi q_s^2/\varepsilon \ , \tag{28}$$

where $\rho_\pm(0)$ are, respectively, the densities of + ions and − ions at the wall, and the Lippmann equation [51,58,65]:

$$\left[\frac{\partial\gamma}{\partial\Delta\Psi}\right]_{\rho_i,T}=-q_s \ , \tag{29}$$

where $\Delta\Psi=\Psi(0)-\Psi(\infty)$ is the potential drop across the double layer and q_s is the uniform charge density on the wall.

In Fig. 12, our results for the reduced density profiles $\rho_i(z)/\rho_i$ are compared with MC data in the "standard" case where a second layer of counter ions is clearly formed. This case corresponds to a 1:1 electrolyte at a bulk concentration $c=1$ M, with $\varepsilon=78.5$, $\sigma=0.425$ nm, $T=298$ K [$\rho\sigma^3=0.0924$, $e^*=(e^2/\varepsilon kT\sigma)^{1/2}=1.2965$] and a very large charge density on the wall $q_s^*=q_s\sigma^2/e=0.7$. There have been several simulations of this system [52–54], which are not in total agreement, especially for the magnitude of the second peak in the counter ion profile and for the value of the potential drop $\Delta\Psi$. We have chosen to compare with the very recent calculations of Caillol and Levesque [54], which have been performed with a new efficient method which avoids the use of the cumbersome periodic boundary conditions by putting the system on the surface of a four-dimensional hypersphere. As seen in Fig. 12, the agreement between theory and simulation is satisfactory, in particular for the position of the second peak in the counter ion profile. The magnitude however is a bit overestimated. On the other hand, we find an overall reduced potential drop $\Delta\Psi^*=e/kT\Delta\Psi=4.49$ (115 mV)

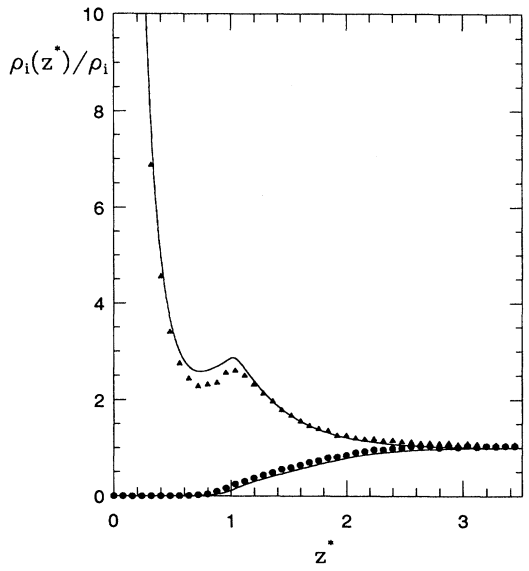

FIG. 12. Ionic density profiles for a 1:1 electrolyte (restricted primitive model with $\sigma=0.425$ nm, $\varepsilon=78.5$, $T=298$ K) near a charged hard wall. The bulk concentration is $c=1$ M and the reduced charge density on the wall is $q_s^*=0.7$. The theoretical results are shown by solid lines, while simulation results (from Ref. [54]) are shown as circles (co-ions) and triangles (counter ions).

which is smaller than the simulation result [54] $\Delta\Psi^*=5.1\pm0.1$ (131 ± 2.6 mV). These performances are comparable to those of Groot's density functional or Tang *et al.* [57] approach in which Tarazona's SDA is extended to the case of hard-sphere mixtures with the same size. Of course the present functional, which is much simpler to implement, is not limited to the RPM and it will be interesting to consider electrolytes (or molten salts) where the anion and cation have very different diameters. Moreover, calculations should be repeated using another theory than the MSA for the bulk properties.

VI. CONCLUSIONS

In this work we have considered several applications of the free-energy density functional proposed in our preceding paper. The aim of the study was to illustrate the versatility of the theory more than to perform a detailed investigation of a specific problem. Therefore, by many aspects, this study is far from being complete. However, we can already state the following conclusions.

(i) Compared to other nonlocal DF theories, the present one seems to be the most adequate to describe packing effects at solid-fluid interfaces and to study the adsorption of simple fluid mixtures at substrates. In all cases considered in this paper, the theory leads to similar or slightly better results than earlier recipes, while requiring a significantly lower computational effort. Its implementation is simple enough that extension to multicomponent mixtures ($n>2$) or polydisperse systems is a straightforward exercise.

(ii) Density-functional methods are now becoming seri-

ous competitors to integral equation theories for the quantitative study of inhomogeneous simple fluids. It is often [5,42] admitted that integral equations based on an approximate closure at the level of the inhomogeneous Ornstein-Zernicke equation are more accurate for the calculation of the one- and two-body distribution functions, while being inadequate for the study of thermodynamic properties. However, we have displayed two examples in Secs. III A and V in which the accuracy of the DF theory is comparable to that of the most sophisticated integral equations. The gain in computational simplicity is considerable.

(iii) The major weakness of existing free-energy functionals is of course the mean-field treatment of the long-ranged attractive part of the interatomic forces. The example given in Sec. IV shows the serious consequences of this approximation for the determination of excess properties in adsorbed phases. Perturbation theory, as suggested by Curtin and Ashcroft [59] and used in Sec. V, may be a way of going beyond this approximation when properties of the corresponding uniform fluid (i.e., pair correlations) are known. On the other hand, the standard WCA separation of the potential, performed in the bulk phase, is also questionable when applied to nonuniform situations where the one-body densities vary significantly. After other authors [22,30], we have verified that choosing a temperature-dependent equivalent hard-sphere diameter, adjusted on the low-temperature liquid-gas coexisting data [31], may improve the predictions of the theory in some cases. However this recipe is not entirely satisfactory because its domain of validity is not clearly delimited. A more systematic procedure should be searched for.

(iv) Density-functional methods—coupled to computer simulations—have already provided a much more detailed insight of adsorption phenomena than the classical thermodynamic description currently in use [66]. Because theoretical studies have so far been limited to highly idealized models for which direct comparison to experiment is not straightforward, it is likely that these thermodynamic methods will not be replaced in the immediate future. However, it is important to realize that for some well-defined real systems, for which experimental data are available, accurate predictions are now reachable. Therefore practical applications of DF theory should be now considered (see, for instance, [67]).

ACKNOWLEDGMENTS

We are grateful to several colleagues for having sent their results or papers before publication: R. Evans, A.R. Denton, and N. W. Ashcroft; Z. Tan and K. E. Gubbins; S. Sokolowski and J. Fischer; J. E. Finn and P. A. Monson; and J. M. Caillol and D. Levesque. Correspondence with P. Monson was particularly helpful. This work was supported in part by the Groupement de Recherche: Centre National de la Recherche Scientifique–Association de Recherche pour les Techniques d'exploitation du Pétrole (wettability) and the FSH (Fond de Soutien des Hydrocarbures).

[1] J. S. Rowlinson and B. Widom, *Molecular Theory of Capillarity* (Oxford University Press, Oxford, 1982).
[2] D. Nicholson and N. G. Parsonage, *Computer Simulation and the Statistical Mechanics of Adsorption* (Academic, New York, 1982).
[3] D. E. Sullivan and M. M. Telo da Gama, in *Fluid Interfacial Phenomena,* edited by C. A. Croxton (Wiley, New York, 1986).
[4] S. Dietrich, in *Phase Transition and Critical Phenomena,* edited by C. Domb and J. L. Lebowitz (Academic, New York, 1988), Vol. 12.
[5] R. Evans, in *Inhomogeneous Fluids,* edited by D. Henderson (Dekker, New York, in press).
[6] R. Evans, J. Phys. Condens. Matter **2**, 8989 (1990).
[7] S. Nordholm, M. Johnson, and B. C. Freasier, Aust. J. Chem. **33**, 2139 (1980); B. C. Freasier and S. Nordholm, J. Chem. Phys. **79**, 4431 (1983); Mol. Phys. **54**, 33 (1986).
[8] P. Tarazona, Mol. Phys. **52**, 81 (1984); P. Tarazona and R. Evans, *ibid.* **52**, 847 (1984); P. Tarazona, Phys. Rev. A **31**, 2672 (1985); P. Tarazona, U. Marini Bettolo Marconi, and R. Evans, Mol. Phys. **60**, 573 (1987).
[9] W. A. Curtin and N. W. Ashcroft, Phys. Rev. A **32**, 2909 (1985); A. R. Denton and N. W. Ashcroft, *ibid.* **39**, 4701 (1989).
[10] T. F. Meister and D. M. Kroll, Phys. Rev. A **31**, 4055 (1985); R. D. Groot and J. P. van der Eerden, *ibid.* **36**, 4356 (1987); S. Sokolowski and J. Fischer, Mol. Phys. **68**, 647 (1989).
[11] T. K. Vanderlick, L. E. Scriven, and H. T. Davis, J. Chem. Phys. **90**, 2422 (1989).
[12] D. M. Kroll and B. B. Laird, Phys. Rev. A **42**, 4806 (1990).
[13] E. Kierlik and M. L. Rosinberg, Phys. Rev. A **42**, 3382 (1990).
[14] Y. Rosenfeld, Phys. Rev. Lett. **63**, 980 (1989).
[15] Y. Rosenfeld, D. Levesque, and J. J. Weis, J. Chem. Phys. **92**, 6918 (1990).
[16] Y. Rosenfeld, Phys. Rev. A **42**, 5978 (1990); J. Chem. Phys. **93**, 4305 (1990).
[17] J. Percus, J. Stat. Phys. **52**, 1157 (1988).
[18] H. Reiss, H. Frisch, and J. L. Lebowitz, J. Chem. Phys. **31**, 369 (1959); E. Helfand, H. L. Frisch, and J. L. Lebowitz, *ibid.* **34**, 1037 (1961).
[19] M. S. Wertheim, Phys. Rev. Lett. **10**, 321 (1963); E. Thiele, J. Chem. Phys. **39**, 474 (1963); J. L. Lebowitz, Phys. Rev. **133**, 895 (1964).
[20] Z. Tan, U. Marini Bettolo Marconi, F. van Swol, and K. E. Gubbins, J. Chem. Phys. **90**, 3704 (1989).
[21] A. R. Denton and N. W. Ashcroft, Phys. Rev. A **42**, 7312 (1990).
[22] B. K. Peterson, K. Gubbins, G. S. Heffelfinger, U. Marini Bettolo Marconi, and F. van Swol, J. Chem. Phys. **88**, 6487 (1988).
[23] E. Kierlik and M. L. Rosinberg (unpublished).
[24] J. Israelachvili, Acc. Chem. Res. **20**, 415 (1987).
[25] R. Evans and U. Marini Bettolo Marconi, J. Chem. Phys. **86**, 7138 (1987).
[26] W. A. Steele, Surf. Sci. **36**, 317 (1973); in *The Interaction of Gases with Solid Surfaces* (Pergamon, Oxford, 1974).

[27] S. Sokolowski and J. Fischer, Mol. Phys. **71**, 393 (1990).
[28] J. D. Weeks, D. Chandler, and H. C. Andersen, J. Chem. Phys. **54**, 5237 (1971).
[29] J. Barker and D. Henderson, J. Chem. Phys. **47**, 4714 (1967).
[30] Z. Tan and K. E. Gubbins, J. Phys. Chem. **94**, 6061 (1990); in *Characterization of Porous Solids II,* edited by International Union of Pure and Applied Chemistry (Elsevier, Amsterdam, 1991).
[31] B. Q. Lu, R. Evans, and M. M. Telo da Gama, Mol. Phys. **55**, 1319 (1985).
[32] L. Verlet and J. J. Weis, Phys. Rev. A **5**, 939 (1982).
[33] E. Bruno, C. Caccamo, and P. Tarazona, Phys. Rev. A **35**, 1210 (1987).
[34] E. Velasco and P. Tarazona, Phys. Rev. A **42**, 2454 (1990).
[35] J. R. Henderson and F. van Swol, J. Phys. Condens. Matter **2**, 4537 (1990).
[36] W. Van Megen and I. K. Snook, Mol. Phys. **54**, 741 (1985).
[37] J. P. R. B. Walton and N. Quirke, Chem. Phys. Lett. **129**, 382 (1986).
[38] J. G. Powles, G. Rickayzen, and M. L. Williams, Mol. Phys. **64**, 33 (1988).
[39] I. K. Snook and W. van Megen, J. Chem. Phys. **72**, 2907 (1980); **74**, 1409 (1981).
[40] J. J. Magda, M. Tirell, and H. T. Davis, J. Chem. Phys. **83**, 1888 (1985).
[41] B. V. Derjaguin, Colloid Polymer Sci. **253**, 492 (1975).
[42] R. Kjellander and S. Sarman, Mol. Phys. **70**, 215 (1990).
[43] J. D. MacElroy and S.-H. Suh, Mol. Phys. **60**, 475 (1987).
[44] Z. Tan, K. E. Gubbins, F. van Swol, and U. Marini Bettolo Marconi, *Proceedings of the Third International Conference on Fundamental Adsorption, Sonthofen,* edited by A. B. Mersmann and S. E. Scholl (Engineering Foundation, New York, 1991); G. S. Heffelfinger, Z. Tan, K. E. Gubbins, U. Marini Bettolo Marconi, and F. van Swol, Mol. Sim. **2**, 393 (1989).
[45] D. M. Ruthven, *Principles of Adsorption and Adsorption Processes* (Wiley, New York, 1984).
[46] D. H. Everett, in *Colloid Science* (Specialist Periodical Reports), edited by D. H. Everett (The Chemical Society, London, 1973), Vol. 1, Chap. 2; C. E. Brown and D. H. Everett, *ibid.*, edited by D. H. Everett (The Chemical Society, London, 1975), Vol. 2, Chap. 2; D. H. Everett and R. T. Podoll, *ibid.*, edited by D. H. Everett (The Chemical Society, London, 1979), Vol. 3, Chap. 2.
[47] A. L. Myers and J. M. Prausnitz, AIChE J. **11**, 121 (1965).
[48] J. E. Finn and P. A. Monson, Mol. Phys. **65**, 1345 (1988).
[49] J. E. Finn and P. A. Monson, in *Proceedings of the Third International Conference on Fundamental Adsorption* (Ref. [44]); Mol. Phys. **72**, 661 (1991).
[50] J. P. Hansen and I. R. McDonald, *Theory of Simple Liquids,* 2nd ed. (Academic, New York, 1986).
[51] S. L. Carnie and G. M. Torrie, Adv. Chem. Phys. **56**, 141 (1984).
[52] G. M. Torrie and J. P. Valleau, J. Chem. Phys. **73**, 5807 (1980).
[53] P. Ballone, G. Pastore, and M. P. Tosi, J. Chem. Phys. **85**, 2943 (1986).
[54] J. M. Caillol and D. Levesque, J. Chem. Phys. **94**, 597 (1991).
[55] C. W. Outhwaite and L. B. Bhuiyan, J. Chem. Phys. **85**, 4206 (1986); C. Caccamo, G. Pizzimenti, and L. Blum, *ibid.* **84**, 3327 (1986); T. Alts, P. Nielaba, B. Daguanno, and F. Forstmann, Chem. Phys. **111**, 223 (1987); R. Kjellander and S. Marcelja, Chem. Phys. Lett. **127**, 402 (1986); M. Plischke and D. Henderson, J. Chem. Phys. **88**, 2712 (1988).
[56] R. D. Groot, Phys. Rev. A **37**, 3456 (1988); R.D. Groot and J. P. van der Eerden, *ibid.* **38**, 296 (1988).
[57] L. Mier-y-Teran, S. H. Suh, H. S. White, and H. T. Davis, J. Chem. Phys. **92**, 5087 (1990); Zixiang Tang, L. Mier-y-Teran, H. T. Davis, L. E. Scriven, and H. S. White, Mol. Phys. **71**, 369 (1990).
[58] R. Evans and T. J. Sluckin, Mol. Phys. **40**, 413 (1980); T. J. Sluckin, J. Chem. Soc. Faraday Trans. II **77**, 575 (1981).
[59] W. A. Curtin and N. W. Ashcroft, Phys. Rev. Lett. **56**, 2775 (1986).
[60] E. Waisman and J. L. Lebowitz, J. Chem. Phys. **56**, 3086 (1972); **56**, (1972).
[61] M. M. Telo da Gama, R. Evans, and T. J. Sluckin, Mol. Phys. **41**, 1355 (1980).
[62] J. S. Hoye, J. L. Lebowitz, and G. Stell, J. Chem. Phys. **61**, 3253 (1974).
[63] L. Blum, J. Hernando, and J. L. Lebowitz, J. Phys. Chem. **87**, 2825 (1983).
[64] D. Henderson, L. Blum, and J. L. Lebowitz, J. Electroanal. Chem. **102**, 315 (1979).
[65] V. Russier, J. P. Badiali, and M. L. Rosinberg, J. Phys. C **18**, 707 (1985).
[66] S. J. Gregg and K. S. W. Sing, *Adsorption, Surface Area and Porosity* (Academic, London, 1982).
[67] N. A. Seaton, J. P. R. B. Walton, and N. Quirke, Carbon **27**, 853 (1989).